Preliminary experimental identification of a FEM human knee model

1st Pasquale Arpaia
Department of Electrical Engineering and Information Technology (DIETI)
University of Naples Federico II
Naples, Italy
pasquale.arpaia@unina.it

2nd Federica Crauso
Department of Biomorphological and Surgical Sciences
University of Naples Federico II
Naples, Italy
federica.crauso@unina.it

3rd Sabrina Grassini
Department of Applied Science and Technology (DISAT)
Polytechnic of Turin
Turin, Italy
sabrina.grassini@polito.it

4th Simone Minucci
Department of Economics, Engineering, Society and Business Organization (DEIm)
University of Tuscia
Viterbo, Italy
simone.minucci@unitus.it

5th Nicola Moccaldi
Department of Electrical Engineering and Information Technology (DIETI)
University of Naples Federico II
Naples, Italy
nicola.moccaldi@unina.it

6th Isabella Sannino
Department of Applied Science and Technology (DISAT)
Polytechnic of Turin
Turin, Italy
isabella.sannino@polito.it

***Abstract*—A customizable Finite Elements Model of human knee is proposed for improving inter-individual reproducibility in NSAIDs transdermal delivery measurement. The model simulates: (i) the measurement system, based on Bio-Impedance Spectroscopy, and (ii) the system under test, namely the knee by five parallel, homogeneous, and concentric layers: bone, muscle, adipose tissue, wet skin, and dry skin. In this paper, first the equations and the architecture of the model are described. Then, the results of the numerical characterization and the preliminary experimental validation are reported. A sensitivity analysis was realized for reducing computational burden during Model customization. Only five parameters out of the 64 used in the Cole-Cole equation were sufficient for fitting experimental data of different subjects.**

***Index Terms*—Finite Element Method (FEM), Electrical impedance spectroscopy (EIS), Bioimpedance, Drug delivery, Biological system modeling, Anatomical structure, Analytic model.**

I. Introduction

The human knee is the largest and most stressed joint in the body, and one of the most commonly injured. A healthy knee is crucial for our optimal daily functions, and influence the quality of life (QOL). Knee pain is a particularly common condition; about 40 million people reporting knee pain, and the incidence increases notably with age. Moreover, the increase of pain severity due to age, could lead to physical disability and decreased QOL [1]. Some of the most common causes of knee pain are: joint or bone injuries, sprains, ligaments strain, tendinitis or degenerative joint disease like osteoarthritis, rheumatoid arthritis and other inflammatory disorders. The therapy recommended for several of these pathologies, often include topical nonsteroidal anti-inflammatory drug (NSAID) use. The NSAIDs, regarded low-cost and nearly safe, were ranked most efficient nonsurgical osteoarthritis knee treatment for enhancing functionality and providing pain relief, as shown in the Journal of the American Academy of Orthopaedic Surgeons (JAAOS) [2]. The NSAIDs are effective analgesics, commonly administered by transdermal drug delivery for the treatment of acute pain and local muscle inflammation. Topical NSAIDs are applied to intact skin in painful area in the form of a gel, cream, spray or patch. These latters (NSAIDs), penetrate the skin, pervade tissues or joints, and reduce the inflammation process with a lower drug levels in the blood compared to the same drug oral administration [3] [4]. A widely used approach to improve transdermal drug delivery is iontophoresis, a type of electrotherapy, a non-invasive, safety and high efficiency method of systemic and local drug delivery exploiting an electric field [5] [6]. At present, there is no acceptable standard method for exactly assessing delivered drug in tissues [7], owing to the intra-individual (different body areas, skin conditions, psychological conditions, and so on), as well as inter-individual factors (sex, age, ethnicity) [8]. Therefore, the absorption kinetics, efficacy, and drug biovailability are poorly understood [9] [10]. Moreover, the evaluation of therapy efficacy and recovery are provided by physical examination of doctors or using expensive, time consuming and harmful diagnostic imaging techniques. Electrical impedance spectroscopy (EIS) has been widely used in biomedical application [11] [12], and especially applied in the field of transdermal drug delivery [13] [14]. EIS, employing a small electrical current, investigates the electrical proprieties of the treated tissue site by measuring its electrical impedance considering the different electrical properties shown by different components of biological tissues [15]. Changes in electrical properties of biological tissues generated by a transdermal drug diffusion are monitored by EIS [16]; beside that, it may provide information on the

skin's reservoir function, crucial to determinate the duration of topical drug action [17], thus enabling the creation of a personalized therapy. In this work, the uncertainty linked to the knee inter and intra-individual variability are dealt with a Finite Element Method (FEM) model. FEM is a very useful Method for the analysis of knee joint, thus, a preliminary knee joint model integrated with subjects specific musculoskeletal parameters was obtained from in-vivo measurements, in order to quantify EIS changes and investigate knee health [18]. After each impedance spectroscopy measurement, the knee model learns the current values of the dielectric parameters of the tissue. In this way it also manages intra-individual factors that can influence the impedance variation such as body temperature or emotional states.
In this paper, the anatomical structure of the knee joint and its dielectric proprieties are presented in II. Meanwhile, proposed knee FEM model is shown in III. Then, the experimental set up is delineated in IV-A and the parameters optimization and customization in IV. Finally, the experimental validation and results are discussed in V

II. Background

A. Knee anatomy

The human knee joint is the largest weight bearing, one of the most complex and most stressed joint in the human body which is located between two longest lever arms. The knee joint is a hinge type joint, which primarily allows for flexion and extension, it connects three bones: femur, tibia and patella. The femur, the thigh bone, is the strongest and longest bone of human body. The proximal part of the femur articulates in hip joint , while the distal part of the femur meets the tibia and patella in knee joint. The tibia, the long anterior leg bone below the knee, connects the knee with the ankle bones [19]. The patella is a flat, triangular bone which covers and protect the anterior surface of the knee joint and, moreover it connects the joint directly to the largest muscle in the human body on the anterior of the thigh: the quadriceps. The quadriceps is a large muscle group In the front of the thigh which extends the knee joint. All articular surfaces are covered with cartilage, a special protective tissue that reduces internal friction in the joint and acts as a shock absorber. Further protection from trauma and wear, is provided by two menisci, the medial and the lateral meniscus. Menisci are thickened semilunar cartilage pad which are crucial for facilitating movements and shock absorption, increasing stability of the joint. The knee joint is surrounded by a joint capsule with four sturdy ligaments: two collateral ligaments placed along the sides of the knee and limit the sideways motion of the knee, while two cruciate ligaments, crossing within the joint, connects the tibia to the femur [20] [21]. The knee anatomy is shown in Fig.1, although numerous other anatomical structures, unmentioned, such as synovial fluid, bursa, minor ligaments, tendons, increase the stability and functionality of the joint [22].

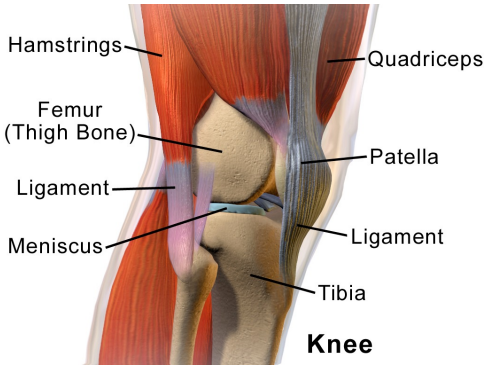

Fig. 1. Knee joint anatomy [22]

B. Dielectric properties of body tissues

From an electromagnetic point of view, biological tissues can be modeled as dielectric materials characterized by either polarization mechanisms and dielectric losses. The polarization mechanisms are generated by an electric charges displacement which needs some time to take place when excited by an external electric field. The dielectric losses are generated by either conduction currents inside the tissue and lossy effects generated by the material polarization.
When exciting the tissues with an external sinusoidal electric field, the dielectric behaviour can be modeled with an electric conductivity, accounting the losses due to free charges conduction, and a complex dielectric function whose real part accounts the polarization of the bound charges and the imaginary part accounts the energy losses due to bound charges and dipole relaxations.
The main characteristics of the frequency spectrum of the dielectric properties of biological tissues were deeply studied over years as reported in [23]; it consists of three main relaxation phenomena, each of them related to a particular polarization mechanism, located in the same number of relaxation regions, namely α, β and γ regions, located at high, medium and low frequency.
Among the numerous models developed to describe the such behaviour, one of the most commonly used for biological tissues is based on the expressions provided by the Cole-Cole model [24]. Cole-Cole equation is a widely used model to describe the relaxation phenomena in dielectrics, obtained by a modification of the Debye relaxation model as follows:

$$\varepsilon_r{}^*(\omega) = \varepsilon_\infty + \sum_n \frac{\Delta\varepsilon_n}{1 + (j\omega\tau_n)^{1-\alpha_n}} + \frac{\sigma_{dc}}{j\omega\varepsilon_0} \qquad (1)$$

where ε_∞ is the value of the dielectric function in the high frequency range (namely in the limit when the angular frequency tends to infinity), σ_{dc} is the static conductivity due to ionic conduction inside the tissue, τ_n is the relaxation time of the n-th relaxation phenomenon, $\Delta\varepsilon_n$ is magnitude of the n-th dispersion, and $0 < \alpha_n < 1$ is an empiric coefficient introduced in the Cole-Cole model which allows to describes

spectral shapes (the higher the value of α the higher the flattening of the spectrum) [23] [25].

III. Proposal

A preliminary model of human knee is proposed in order to monitor NSAIDs bioavailability in transdermal delivery. The exploitation of a numerical model makes it possible to optimize the electrodes design, better evaluate the injuries extent and therapeutics treatments progress. In this section the model and the optimization algorithm, integrated with subjects specific muscoskeletar parameters present in the relevant literature and in-vivo experimental data, are exposed. Useful details for modeling knee joint are the dimensions of human knee bones. Among several studies which deal with this matter, in [26] the measures of human femur and tibia are provided. In Tab. I the typical width of Femur Condyle (FCW), Medial Femur (FW), Tibial Plateau (TPW) and Tibial Plateau Medial (MW) are presented, along with the typical length of Medial Femoral condyle (FL) and Tibial plateau medial (ML) both for male and female are reported. According to further anthropometric studies [27]–[29], the simplified knee geometric structure consists of the femur-tibia-patella articulation enclosed into a multilayered cylinder modeling different tissues, i.e. (from innermost to outermost layer) Muscle, Subcutaneous Fat and Skin. Because of its intrinsic biological layering, the skin layer can be further divided into many sub-layers with different biological characteristics and thickness. In what follows, the skin is divided into two equivalent sub-layers: an internal "wet skin" layer which models the innermost part of the skin (hypodermis and dermis) and an external "dry skin" layer which models the outermost part of the skin (epidermis) [26]. According to the aforementioned anthropometric studies, the thickness of dry skin, wet skin and adipose tissue layers are chosen respectively as follows: 1 mm, 2.7 mm, and 7 mm.
The following Fig.2 and Fig.3 show two sketches of the geometrical structure of the knee articulation and tissues layering.

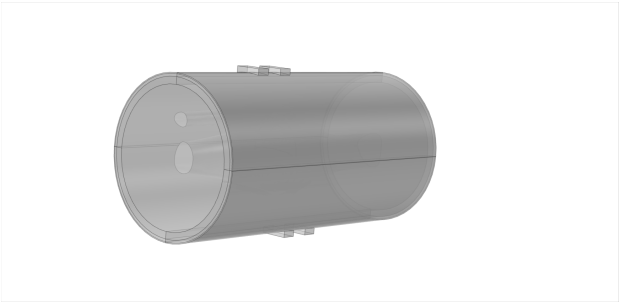

Fig. 2. Knee joint 3D model

After a proper meshing of the whole geometry, the solution of Maxwell equations in the direct current formulation in the frequency domain is afforded via Finite Element Method, in order to evaluate the electric potential phasor in each point of the mesh and the simulated impedance spectroscopy measured by a four-wire device. The boundary conditions to be coupled with the equations are: Dirichlet boundary condition at the current terminals of the simulated measurement device applying the external excitation voltage and Neumann boundary condition on all other surfaces (dry skin and voltage terminals), stating that the normal component of the current density field is zero (electric insulation).
At last, human parameters presented in well claimed study [23] are used to characterize the electrical properties of each tissue, according to Cole-Cole equation, as shown in Tab.II.

Fig. 3. Knee joint 3D model: the particular of bones

TABLE I
Typical human Femur and Tibia dimensions

FEMUR [mm]	GENERAL	MALE	FEMALE
FCW	78,7 ± 6,7	84,2 ± 4,3	73,4 ± 3,6
FL	52,2 ± 4,9	54,3 ± 4,8	50,2 ± 4,1
FW	28,9 ± 3,3	30,6 ± 3,4	27,3 ± 2,6
TIBIA [mm]	GENERAL	MALE	FEMALE
TPW	74,9 ± 6,5	80,6 ± 3,9	69,5 ± 3,0
ML	45,1 ± 4,5	47,9 ± 4,2	42,2 ± 2,9
MW	30,4 ± 3,0	32,8 ± 2,1	28,1 ± 1,4

IV. Model Optimization

For model validation and optimization, in-vivo experimental data, collected during an experimental campaign, were used.

TABLE II
Different tissues parameters value of Cole-Cole equation according to Gabriel [23].

	Dry Skin	**Wet Skin**	**Fat**	**Muscle**	**Bone**
ε_∞	4.0	4.0	2.5	4.0	2.5
$\Delta\varepsilon_1$	32.0	39.0	9.0	50.0	18.0
τ_1 [ps]	7.23	7.96	7.96	7.23	13.26
α_1	0.00	0.10	0.20	0.10	0.22
$\Delta\varepsilon_2$	1100	280	35	7000	300
τ_2 [ns]	32.48	79.58	15.92	353.68	79.58
α_2	0.00	0.00	0.10	0.10	0.25
$\Delta\varepsilon_3$		3.0 x 10^4	3.3 x 10^4	1.2 x 10^6	2 x 10^4
τ_3 [μs]		1.59	159.15	318.31	159.15
α_3		0.16	0.05	0.10	0.20
$\Delta\varepsilon_4$		3.0 x 10^4	1.0 x 10^7	2.5 x 10^7	2.0 x 10^7
τ_4 [ms]		1.592	15.915	2.274	15.915
α_4		0.20	0.01	0.00	0.00
σ_{dc} [S/m]	0.0002	0.0004	0.0350	0.2000	0.0700

A. Experimental set up

Ten health young volunteers (average age 24 years, 30 cm ± 10 cm knee circumference, and 20 kg/m^2 ± 10 kg/m^2 body mass index (BMI)), of whom 7 women and 3 men, were included in the study. The volunteer had not any skin diseases, wounds, inflammation or past knee surgery; moreover, they were asked to avoid the use of moisturizers or oils the measurement day. The informed consent, containing all the information about the experiment, was provided and signed by the subjects. The protocol was explained by the engineer who followed the experimental campaign, then volunteers physiological parameters (sex, age, knee circumference, and BMI) were recorded. The volunteers were asked to sit on a chair completely isolated from the ground by means of a rubber mat. Subsequently, the volunteers were connected to the Drug Under Skin Meter (DUSM), by means of four electrodes. The DUSM was already used by the authors in a previous feasibility study for assessing the volume of drug delivered in a test tissue by impedance measurements [30] [14]. It comes with a 15.0 cm x 17.0 cm x 4.5 cm plastic and aluminium casing; for powering it a USB cable was connected to the laptop, hence the device was never connected to the main supply. EIS was measured by four Electrodes connected to four clips placed on a custom TPU (Thermoplastic Polyurethane) support Fig.4 (b) which ensure a stable measurement set up due to its durability and slightly malleability. The pre-gelled electrodes (FIAB PG500) coated with a bio-compatible gel, were used to facilitate the attachment of the electrodes to the skin surface [31]. Moreover, the laboratory temperature and humidity were monitored during the experiments. Thereafter, the impedance measurement were carried out over 1 Hz - 49 kHz frequency spectrum. The average magnitude of impedance spectroscopy measured on 10 volunteers, represented by dots, is shown in Fig.5. Each experiment was repeated ten times, during 10 s, for each frequency. The 1-σ repeatability, expressed as the relative percentage with respect to the initial impedance value resulted lower than 2%. Therefore, the influence of the dynamic factors (eg blood flow) on the impedance values was considered negligible.

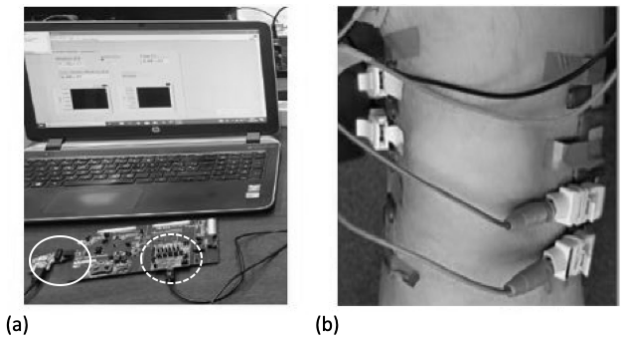

Fig. 4. Experimental set up. The motherboard of DuSM (a) was connected to a laptop PC by the USB-SW/UART-EMUZ (circled with solid line). The daughterboard 4W-BIO3Z (circled with dashed line) was connected to four electrodes on the knee (b) by clip adapters

B. Knee parameters optimization

In order to mitigate the simplifications introduced into the model and the individual variability of the tissues, an optimization procedure is carried out to adapt the values reported in Tab.II to fit the average measured bioimpedance. It consists of three main steps: the first one is the extraction of a subset of parameter from the whole set appearing in Cole-Cole equation, basing on the frequency range spanned by the DUSM to reduce the order of the operational space explored by the sensitivity analysis. Once the parameters subset is identified, the second step is based on a one-at-a-time parameter sensitivity analysis devoted to determine those most affecting the values and the bioimpedance frequency spectrum.
Indication of five electrical parameters to be modified is the output of the sensitivity analysis. Additionally, the static conductivity of the dry skin is considered in the roster of parameters to be optimized in the third step in order to take into account any spectrum modification in the low frequency range.
The aforementioned parameters are used as degree of freedom into an optimization procedure based on the Nelder-Mead simplex method devoted to calculate their optimal value in order to let the shape of the simulated bioimpedance frequency spectrum to fit the measured experimental data.
The goodness of the fit has been evaluated by means of the following figure of merit:

$$\varepsilon_{fit} = \frac{||Z_{meas}(\omega) - Z_{sim}(\omega)||}{||Z_{meas}(\omega)||} \tag{2}$$

where the norm is intended as the eucledean norm of vectors obtained by sampling the measured and the simulated bioimpedance at the DUSM operating frequencies.
The optimization process guarantees the average impedance spectroscopy curve fitting showed in Fig. 5.

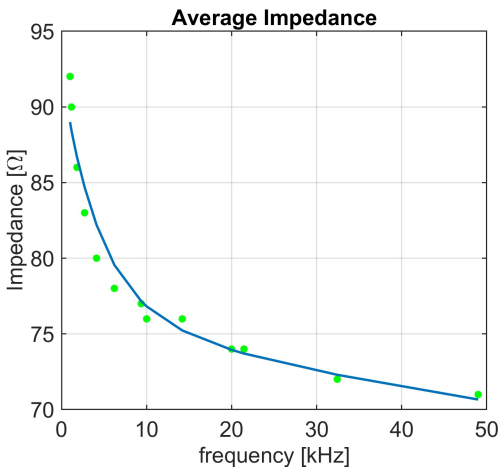

Fig. 5. Model (line) and average experimental (dots) spectroscopy impedance measurements after optimization

C. Sensitivity analysis for model customization

Starting from the output of the optimization process carried out on the average bioimpedance spectroscopy, the same optimization process on the same Cole-Cole parameters was realized for identifying the principal deviations necessary to customize the model for each subject investigated. Four parameter were chosen alongside the subcutaneous fat thickness, dry skin, and muscle in order to distinguish different types of people. Impedance spectroscopy measurements from three volunteers were used for validating the model customization process. The so called *athletic subject* exhibited the lowest impedance values, while the *fat subject* the highest. A third *regular subject* was considered whose impedance values were not far from average. For the *athletic subject* the parameters τ_3, τ_4 of muscle tissue and, σ_{dc} of dry skin became 261.29 x 10^{-6} s, 1.993 x 10^{-3} s, and 0.0006 S/m respectively. Meanwhile, the parameters of muscle τ_3 = 1591.6 x 10^{-6} s, and dry skin σ_{dc} = 0.0001 S/m were changed for *fat subject*. Finally, $\Delta\varepsilon_3$ of subcutaneous fat and τ_3 of muscle became 3.96 x 10^5 and 572.96 x 10^{-6} s for *regular subject*. Results of model customization in term of spectroscopy impedance curve fitting are reported in Fig. 6. In the case of *athletic subject* custom model decreased ε_{fit} by 94% with respect to average model.

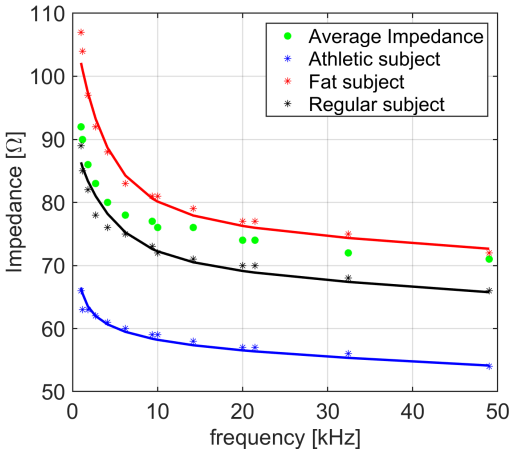

Fig. 6. Customization models for three different subjects

V. Conclusion and Further Works

A customizable FEM model of Knee for improving reproducibility in NSAIDs transdermal delivery measurement was presented. The model geometry was based on five layers: bone, muscle, fat, wet skin, dry skin. The Cole-Cole equation with summation index equal to 4 provided 64 parameters for modeling electrical behavior. Starting from literature and experimental data an *average model* was proposed. A sensitivity analysis was realized for identifying the principal parameters necessary to customize the model. A customizable model based on only five parameters was validated on three subjects. In the case of *athletic subject*, the *custom model* decreased ε_{fit} by 94% with respect to the *average model*. The customization of a knee FEM model with low computational burden was proven feasible. Experimental activities in progress will validate the use of the customizable FEM model for improving inter-individual reproducibility in NSAIDs transdermal delivery measurement.

Acknowledgment

Authors thank D. Cuneo for the support in building the knee FEM model.

References

[1] E. Yelin, S. Weinstein, and T. King, "The burden of musculoskeletal diseases in the united states.," in *Seminars in arthritis and rheumatism*, vol. 46, p. 259, 2016.

[2] D. S. Jevsevar, P. B. Shores, K. Mullen, D. M. Schulte, G. A. Brown, and D. S. Cummins, "Mixed treatment comparisons for nonsurgical treatment of knee osteoarthritis: a network meta-analysis," *JAAOS-Journal of the American Academy of Orthopaedic Surgeons*, vol. 26, no. 9, pp. 325–336, 2018.

[3] S. Derry, P. Conaghan, J. A. P. Da Silva, P. J. Wiffen, and R. A. Moore, "Topical nsaids for chronic musculoskeletal pain in adults," *Cochrane Database of Systematic Reviews*, no. 4, 2016.

[4] F. Rannou, J.-P. Pelletier, and J. Martel-Pelletier, "Efficacy and safety of topical nsaids in the management of osteoarthritis: evidence from real-life setting trials and surveys," in *Seminars in arthritis and rheumatism*, vol. 45, pp. S18–S21, Elsevier, 2016.

[5] J. Zuo, L. Du, M. Li, B. Liu, W. Zhu, and Y. Jin, "Transdermal enhancement effect and mechanism of iontophoresis for non-steroidal anti-inflammatory drugs," *International journal of pharmaceutics*, vol. 466, no. 1-2, pp. 76–82, 2014.

[6] A. Silve, R. Vezinet, and L. M. Mir, "Nanosecond-duration electric pulse delivery in vitro and in vivo: experimental considerations," *IEEE Transactions on Instrumentation and Measurement*, vol. 61, no. 7, pp. 1945–1954, 2012.

[7] R. Sanz, A. C. Calpena, M. Mallandrich, and B. Clares, "Enhancing topical analgesic administration: review and prospect for transdermal and transbuccal drug delivery systems.," *Current pharmaceutical design*, vol. 21, no. 20, pp. 2867–2882, 2015.

[8] P. Clarys, K. Alewaeters, R. Lambrecht, and A. Barel, "Skin color measurements: comparison between three instruments: the chromameter®, the dermaspectrometer® and the mexameter®," *Skin research and technology*, vol. 6, no. 4, pp. 230–238, 2000.

[9] M. Ashford, "Assessment of biopharmaceutical properties," *Aulton's Pharmaceutics E-Book: The Design and Manufacture of Medicines*, p. 339, 2017.

[10] Z. G. Oner and J. E. Polli, "Bioavailability and bioequivalence," in *ADME Processes in Pharmaceutical Sciences*, pp. 223–240, Springer, 2018.

[11] S. Grassini, S. Corbellini, E. Angelini, F. Ferraris, and M. Parvis, "Low-cost impedance spectroscopy system based on a logarithmic amplifier," *IEEE Transactions on Instrumentation and Measurement*, vol. 64, no. 5, pp. 1110–1117, 2014.

[12] F. Clemente, P. Arpaia, and C. Manna, "Characterization of human skin impedance after electrical treatment for transdermal drug delivery," *Measurement*, vol. 46, no. 9, pp. 3494–3501, 2013.

[13] P. Arpaia, U. Cesaro, and N. Moccaldi, "A bioimpedance meter to measure drug in transdermal delivery," *IEEE Transactions on Instrumentation and Measurement*, vol. 67, no. 10, pp. 2324–2331, 2018.

[14] P. Arpaia, U. Cesaro, and N. Moccaldi, "Noninvasive measurement of transdermal drug delivery by impedance spectroscopy," *Scientific reports*, vol. 7, p. 44647, 2017.

[15] B. Tsai, H. Xue, E. Birgersson, S. Ollmar, and U. Birgersson, "Dielectrical properties of living epidermis and dermis in the frequency range from 1 khz to 1 mhz," *Journal of Electrical Bioimpedance*, vol. 10, no. 1, pp. 14–23, 2019.

[16] B. Tsai, H. Xue, E. Birgersson, S. Ollmar, and U. Birgersson, "Analysis of a mechanistic model for non-invasive bioimpedance of intact skin," *Journal of Electrical Bioimpedance*, vol. 8, no. 1, pp. 84–96, 2019.

[17] M. S. Roberts, S. Cross, and Y. Anissimov, "Factors affecting the formation of a skin reservoir for topically applied solutes," *Skin pharmacology and physiology*, vol. 17, no. 1, pp. 3–16, 2004.

[18] N. K. Sahu and A. K. Kaviti, "A review of use fem techniques in modeling of human knee joint," in *Journal of Biomimetics, Biomaterials and Biomedical Engineering*, vol. 28, pp. 14–25, Trans Tech Publ, 2016.
[19] J. F. Abulhasan and M. J. Grey, "Anatomy and physiology of knee stability," *Journal of Functional Morphology and Kinesiology*, vol. 2, no. 4, p. 34, 2017.
[20] S. J. M. Ingham, R. T. de Carvalho, C. A. Martins, P. Lertwanich, R. J. Abdalla, P. Smolinski, C. O. Lovejoy, and F. H. Fu, "Anterolateral ligament anatomy: a comparative anatomical study," *Knee Surgery, Sports Traumatology, Arthroscopy*, vol. 25, no. 4, pp. 1048–1054, 2017.
[21] R. F. LaPrade, A. H. Engebretsen, T. V. Ly, S. Johansen, F. A. Wentorf, and L. Engebretsen, "The anatomy of the medial part of the knee," *JBJS*, vol. 89, no. 9, pp. 2000–2010, 2007.
[22] B. staff, "Medical gallery of blausen medical 2014," *WikiJournal of Medicine*, vol. 1, no. 2, 2014.
[23] S. Gabriel, R. Lau, and C. Gabriel, "The dielectric properties of biological tissues: Iii. parametric models for the dielectric spectrum of tissues," *Physics in Medicine & Biology*, vol. 41, no. 11, p. 2271, 1996.
[24] K. S. Cole and R. H. Cole, "Dispersion and absorption in dielectrics i. alternating current characteristics," *The Journal of chemical physics*, vol. 9, no. 4, pp. 341–351, 1941.
[25] B. Rigaud, J.-P. Morucci, and N. Chauveau, "Bioelectrical impedance techniques in medicine part i: bioimpedance measurement second section: impedance spectrometry," *Critical Reviews™ in Biomedical Engineering*, vol. 24, no. 4-6, 1996.
[26] J. J. Elsner, S. Portnoy, F. Guilak, A. Shterling, and E. Linder-Ganz, "Mri-based characterization of bone anatomy in the human knee for size matching of a medial meniscal implant," *Journal of biomechanical engineering*, vol. 132, no. 10, 2010.
[27] K. Hitt, J. R. Shurman, K. Greene, J. McCarthy, J. Moskal, T. Hoeman, M. A. Mont, *et al.*, "Anthropometric measurements of the human knee: correlation to the sizing of current knee arthroplasty systems," *JBJS*, vol. 85, no. suppl_4, pp. 115–122, 2003.
[28] F. B. Loures, R. J. Carrara, R. F. d. A. Góes, J. M. Barretto, A. Kinder, V. S. Gameiro, E. Marchiori, *et al.*, "Anthropometric study of the knee in patients with osteoarthritis: intraoperative measurement versus magnetic resonance imaging," *Radiologia brasileira*, vol. 50, no. 3, pp. 170–175, 2017.
[29] C. A. McNamara, A. A. Hanano, J. M. Villa, G. M. Huaman, P. D. Patel, and J. C. Suarez, "Anthropometric measurements of knee joints in the hispanic population," *The Journal of arthroplasty*, vol. 33, no. 8, pp. 2640–2646, 2018.
[30] P. Arpaia, O. Cuomo, N. Moccaldi, A. Smarra, and M. Taglialatela, "Non-invasive real-time in-vivo monitoring of insulin absorption from subcutaneous tissues," in *Journal of Physics: Conference Series*, vol. 1065, p. 132008, IOP Publishing, 2018.
[31] A. Asadian, M. R. Kermani, and R. V. Patel, "A novel force modeling scheme for needle insertion using multiple kalman filters," *IEEE Transactions on Instrumentation and Measurement*, vol. 61, no. 2, pp. 429–438, 2011.